

Director structures with dominant in-plane alignment in hybrid planar films of biaxial nematic liquid crystals: A Monte Carlo study.

B. Kamala Latha^{a,*}, G. Sai Preeti^{a,1}, K. P. N. Murthy^{a,2}, V. S. S. Sastry^{a,b}

^a*School of Physics, University of Hyderabad, Hyderabad 500046, India*

^b*School of Engineering Sciences and Technology, University of Hyderabad, Hyderabad 500046, India*

Abstract

Equilibrium director structures in two thin hybrid planar films of biaxial nematics are investigated through Markov chain Monte Carlo simulations based on a lattice Hamiltonian model within the London dispersion approximation. While the substrates of the two films induce similar anchoring influences on the long axes of the liquid crystal molecules (viz. planar orientation at one end and perpendicular, or homeotropic, orientations at the other), they differ in their coupling with the minor axes of the molecules. In Type-A film the substrates do not interact with the minor axes at all (which is experimentally relatively more amenable), while in Type-B, the orientations of the molecular axes at the surface layer are influenced as well, by their biaxial coupling with the surface. Both films exhibit expected bending of the director associated with the ordering of the molecular long axes due to surface anchoring. Simulation results indicate that the Type-A film hosts stable director structures in the biaxial nematic phase of the LC medium, with the primary director lying in the plane of the film. High degree of this stable order thus developed could be of practical interest for potential applications. Type-B film, on the other hand, experiences competing interactions among the minor axes due to incompatible anchoring influences at the bounding substrates, apparently leading to frustration.

Keywords: Hybrid film, Biaxial liquid crystals, In-plane alignment, Monte Carlo simulations

PACS: 64.70.M-, code

1. Introduction

The biaxial nematic phase (N_B) of liquid crystals (LC), predicted theoretically very early [1], and realised experimentally in the past decade, in bent-core [2, 3, 4], tetrapode [5, 6, 7], and polymeric [8, 9] systems, is characterised by a primary director \mathbf{n} and a secondary director \mathbf{m} (perpendicular to \mathbf{n}). Field-induced switching of the secondary director is envisaged to be faster than the primary director in the biaxial nematic phase, a fact which

endows these nematics with a promising potential for use in fast switching electro-optic devices [10, 11]. The orthorhombic N_B phases with D_{2h} symmetry are suggested to be desirable [12] for ready applications.

While the current experimental studies are still concerned with unambiguous confirmation of macroscopic biaxiality [12, 13, 14], theoretical studies have been more optimistic. Modelling the Hamiltonian in terms of interactions among molecular tensors, mean-field predictions within quadratic approximation envisage systems which condense into liquid crystal phases with biaxial symmetry [15, 16, 17, 18, 19]. These encompass molecular structures with wide ranging symmetry [20]. Computer simulations [21] on the other hand have been playing a significant role in investigating these models systematically. Recent Monte Carlo studies based on this lattice model

*corresponding author

¹Present address: Department of Physics, GITAM School of Technology, GITAM University, Hyderabad 500102, India

²Present address: Manipal Centre for Natural Sciences, Manipal University, Manipal 576104, India

focus on the competing effects of different energy contributions in the Hamiltonian on the ordering of the medium [22, 23, 24] in biaxial systems. A molecular dynamics (MD) simulation of the bulk biaxial Gay-Berne fluid under the action of an electric field [25] has convincingly shown that the switching of the director, associated with the minor molecular axes, is an order of magnitude faster than that of the director defined by the long molecular axes.

In the biaxial nematic phase, a different pathway for fast switching between different birefringent states (compared to conventional uniaxial LC systems) is possible because the birefringence can be changed by a rotation of the short axes which are thermally ordered, while the orientation of the long axes could be kept fixed [26]. A possible device configuration to achieve this objective is to use a film of biaxial liquid crystal confined in a planar cell with hybrid boundary conditions, wherein the geometry could constrain the orientation of the primary director (of the long axes) in the biaxial nematic phase, leaving the secondary director (of one of the short axes) free for switching with an appropriate (in-plane) field. Studies on uniaxial hybrid films have established [27, 28] that a bent-director configuration could be realised if the film thickness is greater than a critical thickness determined by the curvature elasticity of the medium and the surface interaction strength. Preliminary work on their biaxial counterpart was carried out earlier [29].

In this context, we investigated the equilibrium director structures in two planar films of biaxial liquid crystals, in the uniaxial and biaxial phases of the medium. The anchoring influences of the two substrates comprising the cell are used to pin the orientation of the primary director [ordering direction of the major (long) axes of the molecules] near the two surfaces so as to result in a bent-director hybrid structure. The substrates can be chosen either not to have influence on the minor axes of the molecules (pure uniaxial coupling with the substrate, say Type-A film), or to couple with the minor axes as well (biaxial coupling with the substrate, say Type-B film). We simulated director structures in both these films based on Markov chain Monte Carlo (MC) sampling technique, constructing corresponding equilibrium ensembles. This paper reports our results examining the role of different anchoring conditions on the orientational ordering in the medium for potential applications.

In section II we introduce the lattice model of the medium, and details of the anchoring conditions of the two films. The MC simulation are also discussed in this section. The equilibrium director structures of the film in the two nematic phases obtained from the computations are depicted and discussed in section III. We also examine the effect of varying the cell thickness, as well as of the relative anchoring strengths at the two substrates, on the director structures in these films. The last section summarizes our conclusions.

2. Model and Simulation details

We consider a planar hybrid film comprising of LC molecules with D_{2h} symmetry. We assign the right-handed triad $\{X, Y, Z\}$ to represent the laboratory-fixed frame and $\{x, y, z\}$ to represent the molecular-fixed frame. We let z direction represent the molecular long axis, while the other two (minor) axes are represented by y and x . The film is obtained by confining the biaxial molecules between two planar substrates taken to be in the X-Y plane. Fig. 1 shows the schematics of a biaxial molecule, orienting influences at the two substrates of the planar film, and the reference axes of the laboratory. The orientational interactions between LC molecules, relevant to the present study, are conveniently accounted for, by adopting a lattice Hamiltonian model wherein the molecules located at the lattice sites are represented by unit vectors in the $\{x, y, z\}$ frame specifying the individual molecular orientations. Within this lattice description, in a film of thickness d the substrate planes are positioned at $Z = 0$ and $Z = d + 1$ (lattice units). The influence of the substrates is simulated by introducing two bounding layers of molecules contained in these planes with the designated, but fixed, orientations, referred to in the literature as ghost molecules [30]. The anchoring conditions in both the films are such that the long axes of the molecules are hybrid-aligned (planar orientation parallel to say, Y -axis at one substrate and homeotropic at the other, parallel to Z -axis). For adequately thick films, the primary director \mathbf{n} is bent satisfying the two incompatible boundary conditions. We distinguish two scenarios: (a) in Type-A film, the ghost molecules interact with the LC molecules in the surface layer anchoring only their long axes, thus implying that the substrate hosts only cylindrically symmetric rod-like LC constituents, and (b) in Type-B film

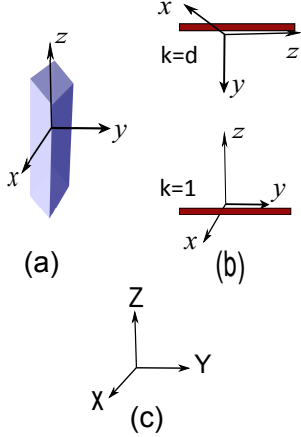


Figure 1: Schematic illustrations of (a) Typical biaxial molecule (b) anchoring directions at the two substrates of the film: homeotropic at the lower ($k=1$) substrate and planar at the top ($k=d$) (c) orientation of the laboratory frame relative to the film.

the ghost molecules themselves have D_{2h} symmetry and interact through a Hamiltonian model appropriate to the biaxial system. These correspond to two qualitatively distinct chemical treatments of the anchoring substrates.

In Type-A film, the molecular z -axes are anchored along the Z -direction in the surface layer near, say, the lower substrate of the cell ($k=1$), while they are kept planar (say, parallel to Y -axis) in other surface layer, near the substrate ($k=d$). As the substrates do not interact with the minor axes of the molecules in this film, they are not, *a priori*, oriented in any specific direction, until guided to equilibrium conditions by the intermolecular and substrate interactions.

In the Type-B film, we impose anchoring conditions of equal strength on all the three molecular axes at each of the two substrates, and use the biaxial Hamiltonian model to account for their interactions with the substrates. The boundary conditions on the film at the two surfaces are summarized as (see Fig. 1):

Substrate 1 at $Z=0$: $z \parallel Z, y \parallel Y, x \parallel X$

Substrate 2 at $Z=d+1$: $z \parallel Y, y \parallel Z, x \parallel X$

2.1. Model Hamiltonian

The biaxial LC molecules are assumed to interact through a pair-wise additive lattice Hamiltonian within

the London dispersion approximation [31], expressed in terms of generalised Wigner rotation matrices as:

$$U(\omega_{ij}) = -\epsilon_{ij}\{P_2(\cos(\beta_{ij})) + 2\lambda_d[R_{02}^2(\omega_{ij}) + R_{20}^2(\omega_{ij})] + 4\lambda_d^2 R_{22}^2(\omega_{ij})\} \quad (1)$$

where $\epsilon_{ij} = \epsilon$ sets the energy scale, and is used to define the reduced temperature, $\omega(\alpha, \beta, \gamma)$ is the set of Euler angles which specify the rotations to be performed in order to bring the reference frame of two molecules i and j in coincidence, R_{mn}^2 are symmetrized Wigner functions, $P_2(\cos(\beta_{ij}))$ is the second Legendre polynomial and λ_d quantifies the biaxial interaction between the molecules. The average values of R_{mn}^2 define the order parameters of the medium in the nematic phases. These are: the uniaxial order $\langle R_{00}^2 \rangle$ (along the primary director), the phase biaxiality $\langle R_{20}^2 \rangle$, and the molecular contribution to the biaxiality of the medium $\langle R_{22}^2 \rangle$, and the contribution to uniaxial order from the molecular minor axes $\langle R_{02}^2 \rangle$ [31]. For simulation purposes, the above Hamiltonian is recast in the Cartesian form, as

$$U = -\epsilon\{\frac{3}{2}V_{33} - \sqrt{6}\lambda_d(V_{11}-V_{22}) + \lambda_d^2(V_{11}+V_{22}-V_{12}-V_{21}) - \frac{1}{2}\}. \quad (2)$$

Here, $V_{ab} = (u_a \cdot v_b)^2$, and the unit vectors u_a, v_b , [$a, b = 1, 2, 3$], are the three axes of the two interacting neighbouring molecules. λ_d sets the relative importance of the biaxial interaction in the Hamiltonian, while ϵ (set to unity in the simulations) defines the temperature scale ($T' = \frac{k_B T^*}{\epsilon}$), where T^* is the laboratory temperature in Kelvin.

This model in a bulk system was studied extensively both through mean-field analysis and MC simulations based on Boltzmann sampling methods. The value of λ_d for the present study is kept at 0.35, keeping in view the high degree of biaxiality it induces, as well as the convenience of a wider biaxial nematic range of temperature made available for our study [31].

2.2. Simulation Details

A planar hybrid film of (lattice) dimensions $15 \times 15 \times d$ ($d = 6, 8, 10, 12$ layers) is considered in the present work.

Periodic boundary conditions are applied along the laboratory X and Y directions, so as to minimize finite size effects. The anchoring conditions applied at the two substrates (contained in the X-Y plane) depend on the specific choice of the film (Type A or B), and their relative strengths are chosen as desired. We index the LC layers with k , starting from the substrate imposing homeotropic anchoring influence on the long molecular axes. The LC ghost molecules in the substrate layers (which are adjacent to the two bounding layers of the LC medium) do not participate in the Monte Carlo dynamics. The interaction strengths of the long molecular axes at the two substrates are represented by ϵ_1 and ϵ_d . ϵ_1 is set equal to one and ϵ_d is varied relative to ϵ_1 , taking values 0.1, 0.2,1.0. The strong anchoring case corresponds to $\epsilon_1 = \epsilon_d = 1$ at the substrates. All simulations except those involving the explicit variation of the relative anchoring strengths (Section 3.4), are carried out under strong anchoring conditions. The temperature T' (in dimensionless units) is set by the coupling strength ϵ in the Hamiltonian (Eqn.1).

The simulation always starts from an initial (random) configuration and the Markov chain dynamics is effected by random moves in the configuration space, accepted or rejected as per the Metropolis algorithm. This Monte Carlo procedure ensures that the system is attracted eventually to its basin of equilibrium states consistent with the simulation conditions. Attainment of equilibration is borne out by the stationarity of the properties of the system, like energy; in equilibrium their fluctuations are centered about a constant mean value. In each simulation, the reduced temperature is varied from 2 to 0.05 in steps of 0.005, and at each temperature the film has been found to be well equilibrated after 5×10^5 lattice sweeps (attempted moves over all the sites). Data from the resulting canonical ensembles are collected over a production run of 5×10^5 lattice sweeps yielding acceptably small sampling errors. The physical properties computed are the average values of energy E , the specific heat C_v , the order parameters $R_{00}^2, R_{02}^2, R_{20}^2, R_{22}^2$ [31, 32] and their susceptibilities. (The susceptibility of the order parameter, say X , at temperature T' is computed as $(\langle X^2 \rangle - \langle X \rangle^2)/T'$). The layer-wise orientation of the local directors corresponding to the molecular z -axes (orientation averaged over the layer) with respect to the laboratory Z-axis (polar angle θ , layerwise) as well as the angle made by this local layer-wise director with respect to laboratory X-axis

(azimuthal angle ϕ , layerwise) are also presented. We computed both layer-wise properties (to examine this director structure and its relative changes) as well as the bulk film properties (averaged over the sample), as a function of temperature, for a fixed relative anchoring strength and layer thickness. The simulations are then repeated by varying the thickness effecting the length scale of the system, and also varying the anchoring strength (ϵ_d) to look for possible anchoring-induced transitions among the different director structures (Sections 3.3 and 3.4).

Errors from finite sizes of the MC samples are estimated employing resampling methods based on the jackknife (JK) algorithm [33, 34]. For this purpose, the total number of sampled data (5×10^5) is divided into 1000 subsets, each consisting of 500 contiguous microstates. The physical quantities of interest are averaged over each of these subsets, yielding 10^3 data points for each variable. The JK algorithm is applied to this reduced data set, to compute the averages and sampling errors. This resampling technique is known to reduce artefacts that could arise due to probable correlations in the original sampled data.

3. Results and Discussion

Fig. 2(a) depicts the variation of specific heat and the two major order parameters in a bulk biaxial fluid (without confinement) of comparable dimensions ($15 \times 15 \times 15$) computed based on MC simulations under periodic boundary conditions, using the above dispersion Hamiltonian model at $\lambda_d=0.35$. The two peaks in the specific heat at $T_1 = 1.123$ and $T_2 = 0.571$ indicate the high temperature $I - N_U$ and low temperature $N_U - N_B$ phase transitions [31]. The phases, as identified by the Metropolis-based Boltzmann sampling procedure employed here, are marked by the progressive growth of the uniaxial order R_{00}^2 and the biaxial order R_{22}^2 , as a function of temperature, bringing out the onset of the uniaxial phase N_U and low temperature biaxial phase N_B . The variation of R_{02}^2 and R_{20}^2 with temperature, as shown in Fig. 2(b), is the expected variation in the bulk system. Figs. 3 - 8 show the simulation results for Type-A and Type-B films of thickness $d = 8$ under strong anchoring conditions ($\epsilon_1 = \epsilon_d = 1$). Fig. 3 shows the onset of the ordering at the $I - N_U$ and $N_U - N_B$ transitions (system properties) in the Type-A film. Fig. 4 provides variation of all

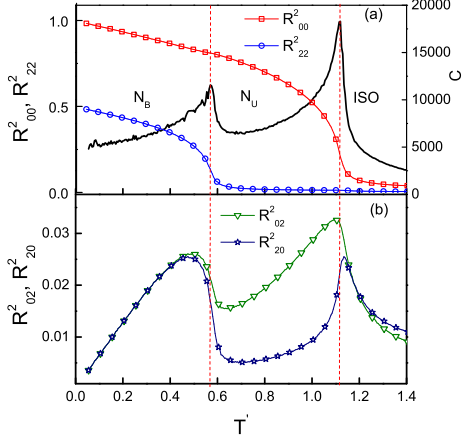


Figure 2: Variation with temperature of system properties a bulk biaxial film ($15 \times 15 \times 15$): specific heat C_v peaks mark the phase transitions $I-N_U$ and N_U-N_B . The temperature variation of the order parameters(a) R^2_{00} , R^2_{22} (b) R^2_{02} and R^2_{20} can be clearly observed.

the four order parameters and their susceptibilities in the Type-A film, averaged over the sample. The qualitative difference between the thermal evolution of these order parameters in the bulk and Type-A film (in particular R^2_{00}) may be noted for further discussion later. The director structure in the film is better appreciated by focussing on the ordering tensor of the molecular z -axes and examining its degree of ordering in each layer and the orientation of the corresponding local layer director with respect to laboratory axes, specified by their θ and ϕ . These layer-wise properties are shown for Film-A in Fig. 5. Similar data were obtained for Film-B as well, and are represented in Figs. 6 - 8, respectively. It is to be noted that layer-wise angles of the local directors are obviously not meaningful in the isotropic phase, and hence such information in these figures (Figs. 5 and 8) (generated automatically during computations) are to be ignored; such data are relevant only in the ordered phases.

Error estimates of different physical properties (energy, R^2_{00} and R^2_{22}) are presented in Table 1 for both the films. Two representative temperatures as indicated are chosen in the two nematic phase, and the averages as well as errors (from the JK algorithm) are shown in the Table. These are sampling errors from a single production run, representing standard deviation of the corresponding MC

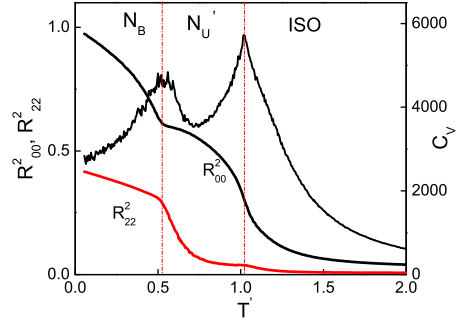


Figure 3: Variation with temperature of system properties in Type-A film. Specific heat C_v peaks mark the phase transitions $I-N'_U$ and N'_U-N_B . The bent - director structure of uniaxial order parameter R^2_{00} in the uniaxial phase is visible clearly.

mean values. As may be seen, they are too small to be shown along with symbols (representing the data points) in the figures. These values indicate that the corresponding MC estimates are robust in terms of their reliability. We further tested whether different trajectories originating from distinct random initial configurations (say, ten such initial conditions) would lead to the comparable values of MC estimates within these errors, to confirm the uniqueness (or otherwise) of the free energy minimum (with respect to the different observables). We carried out such MC simulations on both these films over the temperature region and estimated the standard deviation of the MC values over these trajectories. These show that in Type-A film the error arising from scatter of the MC averages from different simulations are comparable, and are of same order of representative JK errors from a single MC simulation. This indicates a unique, fairly deep, free energy minimum in Type-A in both the nematic phases. Such a comparison in Type-B film shows that the free energy minimum seems to be similar in the intermediate phase, but not in the biaxial phase. The larger scatter from different trajectories in the biaxial phase betrays a shallow free energy minimum with respect to the order parameter; there appear to be several local minima, forming basins of attraction for different starting initial conditions. These observations on errors are relevant for later discussion.

Table 1: Typical errors of computation in the two films, as estimated from a single MC production run of 10^5 data points, with the jack-knife method

Physical variable	Average values with error estimates			
	N'_U phase ($T = 0.7$)		N_B phase ($T = 0.2$)	
	Type-A	Type-B	Type-A	Type-B
Energy per lattice site	-2.398 ± 0.0003	-2.415 ± 0.0002	-3.484 ± 0.0001	-3.492 ± 0.0001
R_{00}^2	0.567 ± 0.0003	0.535 ± 0.0002	0.903 ± 0.0001	0.837 ± 0.0004
R_{22}^2	0.090 ± 0.0006	0.042 ± 0.0003	0.387 ± 0.0001	0.434 ± 0.0001

3.1. Type-A Film

We note at the outset that in this film the substrate interacts with only the long axes of the molecules, while LC molecules themselves have biaxial interaction among them. This system (Fig. 3) undergoes two transitions at $T_1 = 1.021$, and the second at $T_2 = 0.525$, both being lower than the corresponding temperatures in the bulk system (see Fig. 2). Keeping in view the significant biaxial order developed in the films even in the intermediate phase and recognising that its origin is the spatial (layer-wise) inhomogeneities in the ordering tensors of individual layer structures (with respect to the dominant director from the ordering of the molecular z -axes), we refer to this as N'_U phase (rather than N_U), in line with the nomenclature in vogue to denote such uniaxial phases hosting inhomogeneous regions of biaxial order [35].

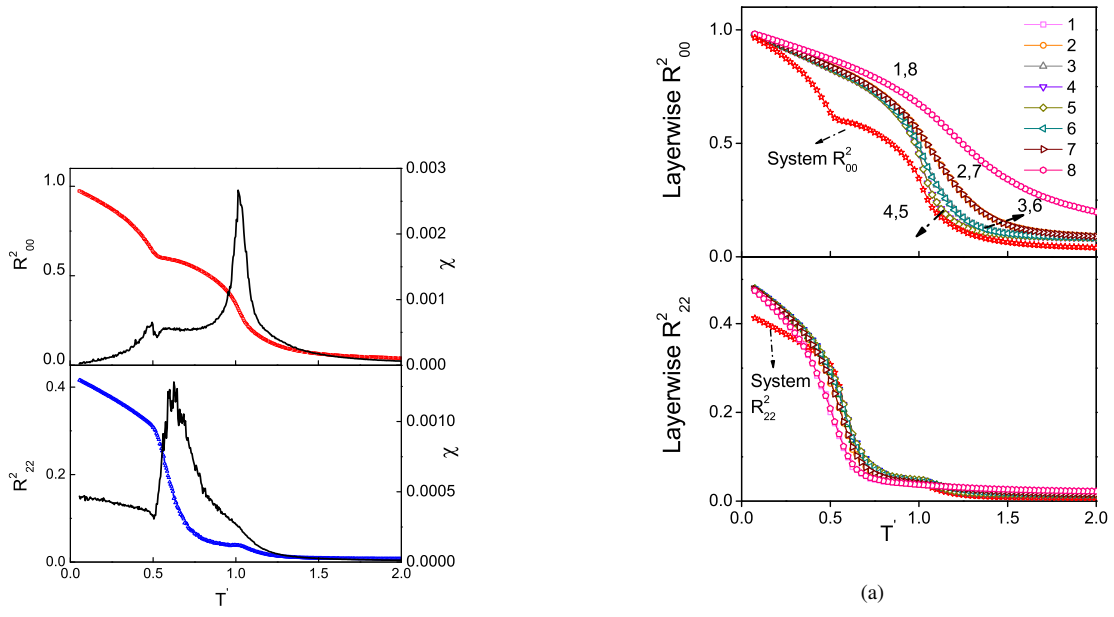
Figs. 4(a) and 4(b) show the four order parameters of the system along with their susceptibilities. It is observed from Fig. 4(a) that the R_{00}^2 susceptibility profile, which is a measure of the fluctuations in the long-range order of the primary director, shows two peaks. The larger peak (at T_1) corresponds to rapid increase of R_{00}^2 in the uniaxial nematic phase. The R_{00}^2 curve displays a bent-director structure and attains a maximum value of 0.6 in this phase. The smaller peak close to T_2 signals a sudden change in the slope of the R_{00}^2 curve leading to a steady increase of the dominant (uniaxial) order towards a maximum value of unity, deep in the biaxial phase. The susceptibility of the biaxial order, on the other hand, shows a single broad peak at a temperature slightly higher than T_2 , signalling

the onset of biaxial order in this phase.

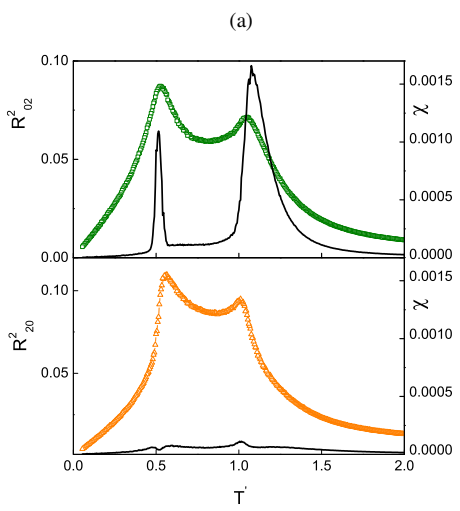
Contribution to the ordering along the uniaxial director originating from molecular minor axes, R_{02}^2 and the phase biaxiality parameter arising from the non-cylindrical distribution of the molecular long axes around the primary director, R_{20}^2 are shown in Fig. 4(b). As compared to their values in a bulk system (Fig. 2), these parameters have larger values in the N'_U phase, - a manifestation of the geometric confinement.

The layer-wise variations (for the layer index $k = 1$ to d) of properties connected with director structures, plotted along with the corresponding bulk values of the film (sample averages) are shown in Figs. 5(a) - 5(c). It is observed from Fig. 5(a) that layer-wise R_{00}^2 values vary smoothly, unlike the abrupt jump at T_2 exhibited by the sample average. Further, the order values in all the layers asymptotically reach the maximum value of 1.0 at the lowest temperature. The variation also shows that the middle layers ($k = 4$ and 5), being the least influenced by the substrate boundaries, are most effective in contributing to the critical onset of the order at the transition. The sample average and layer-wise behaviour of biaxial order shows that in the middle layers R_{22}^2 starts increasing from the $I - N'_U$ transition itself, but a significant increase is observed only at the $N'_U - N_B$ transition. The layer-wise R_{02}^2 and R_{20}^2 are shown in Fig. 5(b). It is observed that they continue to be relatively insignificant.

The plots of the layer-wise θ and layer-wise ϕ are shown in Fig. 5(c). Focusing on the data only below the clearing point, it is observed that as the temperature

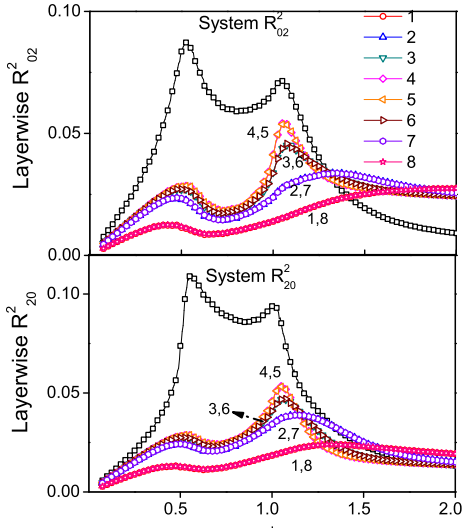


(a)

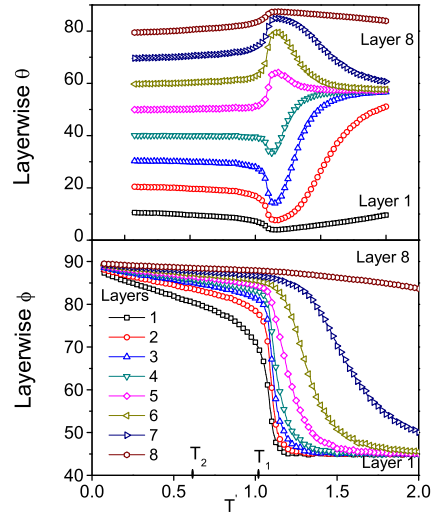


(b)

Figure 4: Variation with temperature of the four system order parameters (lines with symbols) and their susceptibilities (continuous lines) in Type-A film (a) R^2_{00} and R^2_{22} (b) R^2_{02} and R^2_{20} .



(a)



(b)

is lowered from the isotropic phase, layer-wise θ values stabilise at certain fixed values in the intermediate phase. The value of this angle increases monotonically from $k = 1$ layer to the $k = d$ layer, clearly indicating that the layer-wise primary director (of this phase) bends gradually from the lower substrate to the upper substrate, corresponding to the expected bent-director structure. The layer-wise ϕ angles show a sudden flip by approximately 90° just below the $I - N'_U$ transition, particularly in the region of middle layers, pointing to the onset of the dominant order essentially confined to the laboratory YZ plane, as the system is cooled. The profile of the layer-wise angle also suggests that this bent-director structure is not affected by the $N'_U - N_B$ transition.

3.2. Type-B Film

The simulations of the Type-B film were carried out similarly using different anchoring conditions at the substrates, as mentioned earlier. We note that in this film the interaction between the substrate and the surface film layers is biaxial in nature, similar to the interaction between the LC molecules in the bulk. This system undergoes two transitions at $T_1 = 1.014$, and the second at $T_2 = 0.527$, exhibiting the sequence $N_B - N'_U - I$ (see Fig. 6). Introduction of biaxial coupling between the substrates and the surface film layers, in the presence of an already constrained bent director of the molecular z -axes, introduces incompatible boundary conditions on the minor axes as well, and seem to lead to interesting manifestations.

Referring to Fig. 6, it may be noted that the the degree of biaxial order in the intermediate phase (N'_U) is relatively smaller than in the same phase of Type-A film (Fig.3). Figs.7(a) and 7(b) show the temperature variation of the order parameters and their susceptibilities. Interestingly, the dominant order R_{00}^2 and its susceptibility exhibit large fluctuations in the biaxial nematic phase, unlike in Type-A film.

The system and layer-wise variations of different order parameters are shown in Figs. 8(a) - 8(b). The layer-wise R_{00}^2 values in Fig. 8(a) do not fluctuate in the biaxial phase and attain maximum ordering, interestingly unlike the system order parameter. The layer-wise biaxial order shows a non - zero value just below the $I - N'_U$ transition and grows gradually, while the system biaxial order develops more appreciably at the $N'_U - N_B$ transition. Both fluctuate significantly in the biaxial phase similar to the

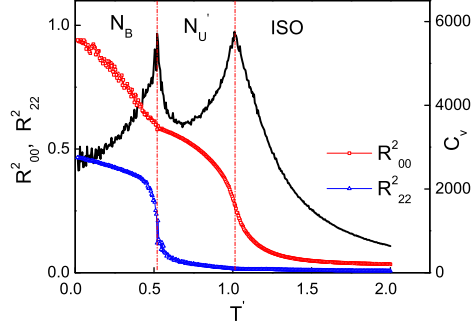
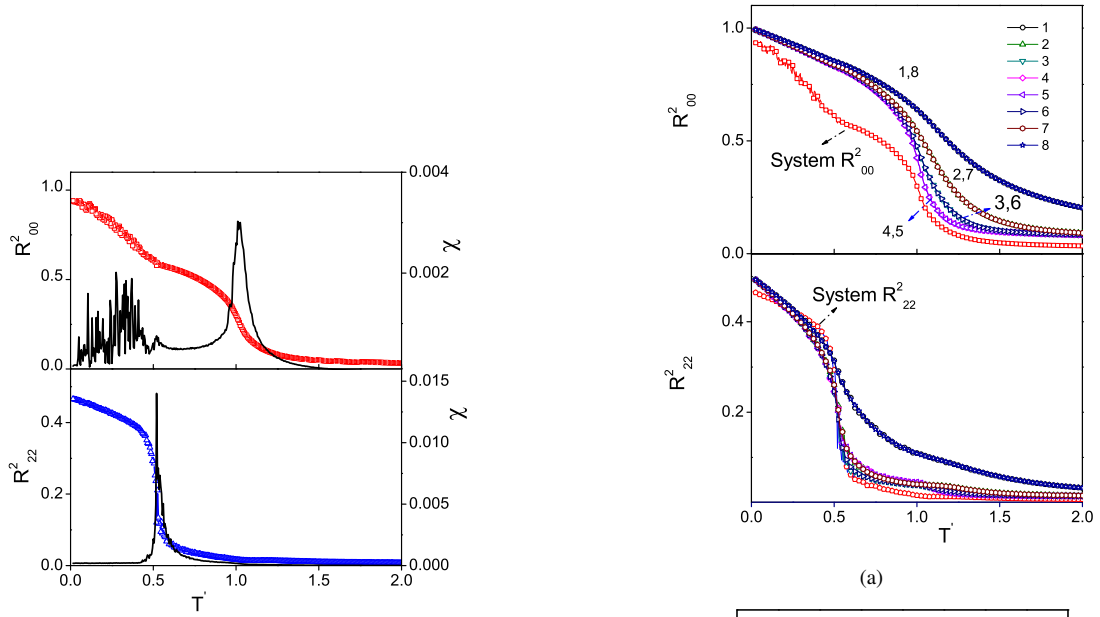


Figure 6: Variation with temperature of system properties in Type-B film - peaks of the specific heat C_v mark the phase transitions $I - N'_U$ and $N'_U - N_B$. The phases are identified by the growth of the major order parameters R_{00}^2 and R_{22}^2 .

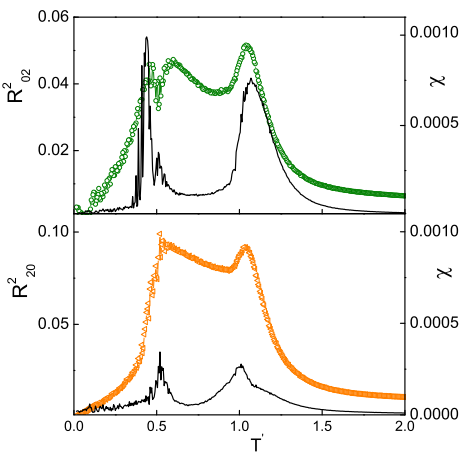
other order parameters. The layer-wise R_{02}^2 and R_{20}^2 shown in Fig. 8(b) have small, nonzero values in the intermediate phase, they also fluctuate more in the biaxial phase.

The layer-wise θ and ϕ values shown in Fig. 8(c) depict variations with temperature in the two nematic phases, which are largely similar to the behaviour of Type-A film, but for significant fluctuations on the onset of the $N'_U - N_B$ transition. It again appears that the layer-wise magnitudes of the two dominant orders are relatively stable, but their orientations are not.

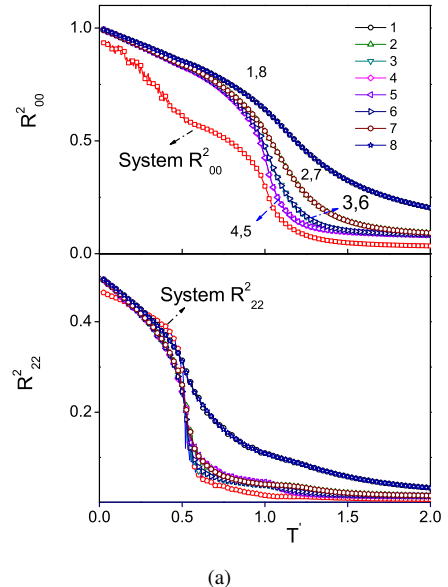
Typical (low) errors quoted in Table 1, particularly in the case of R_{00}^2 in biaxial phase of Type-B film, cannot account for its large fluctuations, discernible by its non-smooth variation with temperature in this phase. We investigated the possible origin of these fluctuations by comparing the results of distinct MC simulations on both the films covering the temperature range, starting with ten different initial random configurations. We examined the statistics of the resultant averages (of corresponding quantities in the different phases), arising from different trajectories in the configuration space. We find that the JK errors from MC simulations over different trajectories are comparable in each of these films at corresponding temperatures, and as small as indicated in Table 1. However the scatter of the MC averages of order parameters, in particular R_{00}^2 , of Type-B film in its biaxial nematic phase, is much larger than any of its single trajectory JK estimates. The standard deviation of the average R_{00}^2 value in this



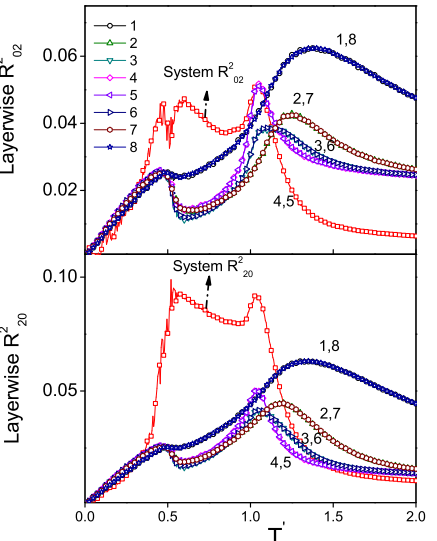
(a)



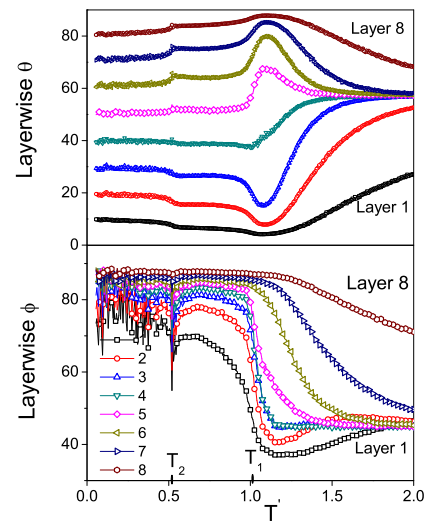
(b)



(a)



(b)



(c)

Figure 7: Variation with temperature of the four system order parameters (lines with symbols) and their susceptibilities (continuous lines) in Type-B film (a) R^2_{00} and R^2_{22} (b) R^2_{02} and R^2_{20} .

phase of Type-B film, obtained from the different trajectories is typically 1×10^{-3} , large compared to the single trajectory JK error of 1×10^{-4} . This points to the scenario that the biaxial nematic phase of Type-B film does not host a single unique free energy minimum, but is rather shallow with many local minima, to which each of the trajectories is attracted depending on the initial conditions. This seems to account also for the fluctuation of the order parameters (and their susceptibilities) in this phase. We will return to this point later in the text.

We now discuss the evolution of the sample uniaxial order (R_{00}^2) in the two films as the system transits through the two transitions, specifically in comparison with the layerwise behaviour (Figs. 5(a), 8(a)). Focussing on Type-A film initially, we note that the sharp increase in this order at the $N'_U - N_B$ transition is unlike the variation in the bulk sample (Fig. 2), and is not supported by its layerwise variations. The latter are smoothly varying across the transition, and the director angles (θ, ϕ) also do not betray the presence of an intermediate phase transition. And yet, the bulk order of the film, defined and computed as corresponding to the maximum eigen value of the ordering tensors of the three molecular axes, is very sensitive to this transition. The case of the Type-B film is qualitatively the same, but for the onset of significant fluctuations in the N_B phase at T_2 . This points to the need to further investigate this system in terms of thermal variations of the eigen values of the three axes separately and examine their behavior across this transition.

Accordingly, we computed equilibrated averages (over the film) of the maximum eigen values (q_x, q_y, q_z) of the ordering tensors (Q_{xx}, Q_{yy}, Q_{zz}) of the three molecular axes and we depict their variation for the case of Type-A film in Fig. 9(a). We also show the directions (θ, ϕ) of the corresponding three eigen vectors, as a function of MC steps after equilibration, in the N_B phase, in Fig. 9(b). From these two figures, it is evident that the onset of the biaxial phase in this confined system (at $T_2=0.5$) leads to a sudden change in the direction of dominant order of the film itself. While the alignment of the long molecular axes defines the primary director till T_2 , it is the molecular y axes which are the most ordered among the three, below this temperature. In conjunction with Fig. 9(b), we see that the ordering direction of this axis is indeed in the laboratory X-direction in the biaxial phase, while the other two eigen vectors are confined to the laboratory

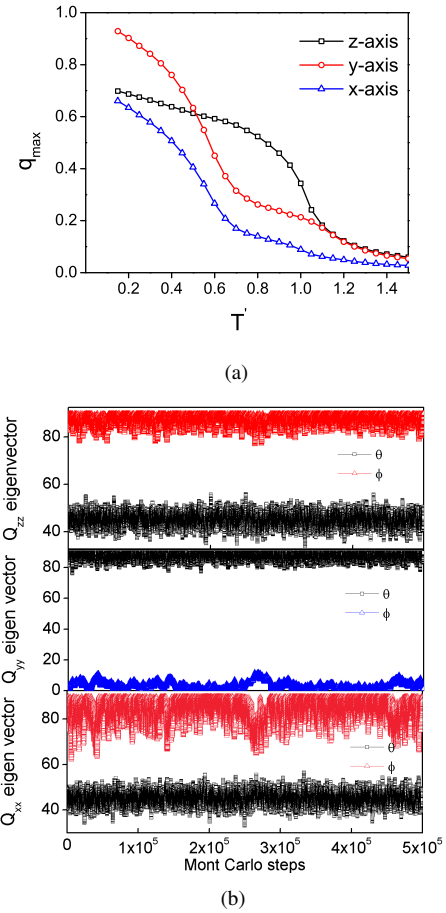


Figure 9: Type-A film : (a) Variation of maximum eigen values (q_{max}) associated with each of the ordering tensors of the three molecular axes (x, y, z), as a function of temperature; (b) The orientations of the corresponding eigen vectors plotted as a function of the Monte Carlo steps after equilibration, at temperature $T = 0.5$ below the $N'_U - N_B$ transition temperature.

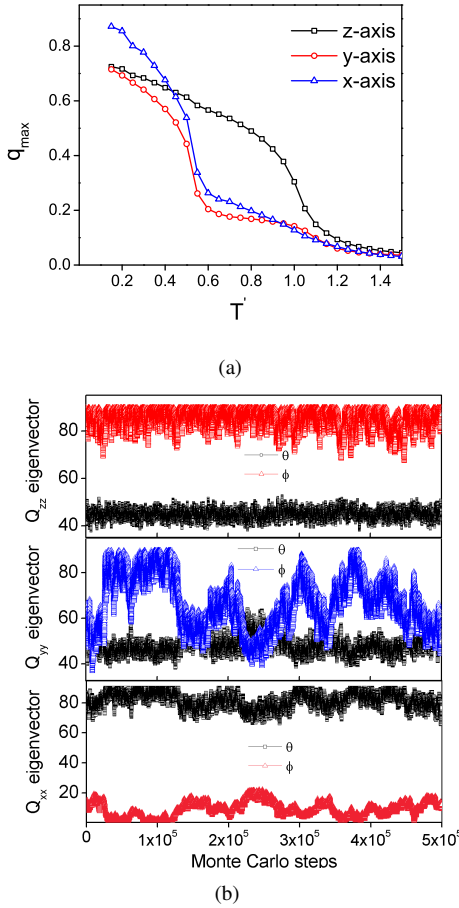


Figure 10: Type-B film : (a)Variation of maximum eigen values (q_{\max}) associated with each of the ordering tensors of the three molecular axes (x, y, z), as a function of temperature; (b) The orientations of the corresponding eigen vectors plotted as a function of the Monte Carlo steps after equilibration, at temperature $T = 0.5$ below the $N'_U - N_B$ transition temperature.

YZ plane, mutually perpendicular to each other. It may be noted that the onset of a biaxial phase thus leads to maximal ordering of the second major axes, wholly contained in the plane of the substrate, and the anchoring conditions imposed in this case constrain the molecular x -axes and z -axes due to anchoring effects, leaving the y -axis to freely develop significant order in the plane of the film.

In contrast, Type-B film which imposes anchoring restrictions on the minor axes of molecules as well at both the ends, presents a very different scenario. We refer to Fig. 10(a) showing (q_x, q_y, q_z) as a function of temperature in this film. At the onset of the second transition at $T_2 \sim 0.51$, q_z (~ 0.617) is higher than the q_x (~ 0.536) and q_y (~ 0.447). However on further cooling, q_x crosses the value of q_z (~ 0.632 at $T' = 0.433$), while q_y remains less than q_z . At lower temperatures q_x saturates at ~ 0.87 , while q_y and q_z saturate to a value of ≤ 0.72 . Eigen vector of q_z makes an angle $\theta \sim 45^\circ$ with the laboratory Z-direction and $\phi \sim 90^\circ$ with laboratory X-direction, thereby indicating that the bent-director structure originating from the ordering of the molecular z -axes is contained in the YZ plane, as is also the case in the high temperature nematic phase. Curiously the eigen vector of q_y is oriented at angles $\theta \sim 45^\circ$ and with a fluctuating ϕ varying between 0° to 90° (see Fig. 10(b)). The maximal ordering direction in this film is determined by the ordering tensor of the molecular x -axes and its azimuthal angle ϕ is eventually contained in the plane of the substrate pointing to the laboratory X-direction. It may be noted that the corresponding fluctuations of the azimuthal angle ϕ of the local directors of the x and y molecular axes are complementary (Fig. 10(b)).

It is now clear that the observed significant fluctuations in the thermal averages, particularly of R_{00}^2 at the onset of the N_B phase, arises due to the fluctuations in the directions of the different ordering tensors (Figs. 7(a) and 7(b)). The qualitatively different scenario of the Type-B film, relative to Type-A, seems to arise due to the imposition of additional restrictions on all the molecular axes at the two substrates.

Comparing the two films in their biaxial phase, we observe that both have primary director (defined as the direction of maximum molecular order) contained in the plane of the substrates, with molecular y -axes defining such a direction for the Type-A film while x -axes play that role for Type-B film. However, imposition of anchoring con-

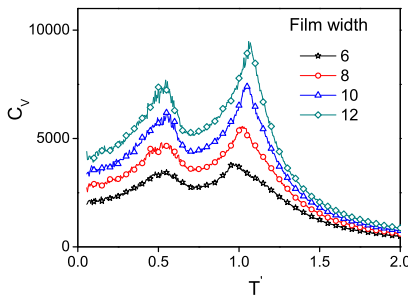


Figure 11: Comparison of variations of the specific heat C_v as a function of temperature in films of thickness d (in lattice units) = 6 (stars), 8 (circles), 10 (upward triangles) and 12 (diamonds), in Type-A film.

straints on all molecular axes leaves the second film frustrated, leading to significant fluctuations of the ordering directions. It is in this context that the earlier observation on the scattering of the MC average values arising from different initial random configurations points to a glass-like behaviour of the frustrated Type-B film, once the onset of its biaxial phase takes place.

From a practical point of view, it is simpler to prepare substrates which need to restrain only one type of axes of the system. Thus Type-A lends itself as a possible stable structure containing significant order within the plane of the film, with potential applications.

3.3. Effect of thickness

We examined the effect of varying the thickness ' d ' in both films, ($d = 6, 8, 10, 12$ lattice units), while retaining the same lateral dimensions, and strong anchoring conditions at the two substrates. Figs. 11 and 12 show this effect on the specific heat C_v and the order parameters R_{00}^2 , R_{22}^2 , R_{02}^2 and R_{20}^2 in the Type-A film, while Figs. 13 and 14 depict the variations for a Type-B film, respectively.

Type-A film It is observed from Fig.11 that the specific heat profiles of the Type-A film become sharper as the thickness increases (size effect). The order parameter variations shown in Fig.12 show that the uniaxial order parameter R_{00}^2 increases marginally in the uniaxial phase as the thickness increases, retaining its bent director structure for all thicknesses. The biaxial order R_{22}^2 shows a slight decrease as the thickness increases and shows a

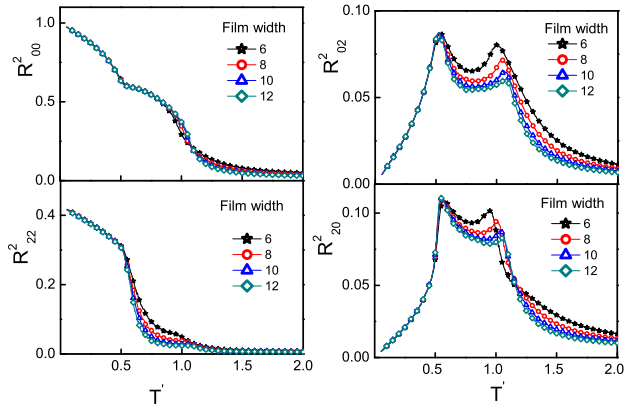


Figure 12: Comparison of variation of order parameters with temperature for different film thickness (d) in Type-A film; $d = 6$ (stars), $d = 8$ (circles), $d = 10$ (upward triangles) and $d = 12$ (diamonds)

marked increase in the temperature of the nematic phase itself for a thinner film ($d=6$). The R_{02}^2 and R_{20}^2 values decrease as the thickness increases. These observations indicate that the gross features of director structures in Type-A film are relatively insensitive to the film thickness, alluding to some degree of flexibility in its design.

Type-B film The effect of varying the thickness of the Type-B film on the specific heat profiles (Fig. 13) and the order parameters (Fig. 14) is similar to Type-A film, except the biaxial order. The variation of R_{22}^2 is independent of the film thickness unlike the other order parameters. The data in the biaxial phase of this film however suffer from large fluctuations at all thickness values.

3.4. Effect of anchoring strength

We further examined both the films (at fixed thickness $d = 8$) with respect to a change in the anchoring strength ϵ_d at the surface layer. We relax the strong anchoring condition ($\epsilon_d = 1$) and vary its value now from 0.0 to 0.6 in steps of 0.1, and compute equilibrium averages (as a function of temperature) of the four order parameters. We depict their dependence on ϵ_d in Figs. 15 and 16 for Type-A and Type-B films, respectively. The other simulational conditions remain the same as before.

We observe from Fig. 15(a) and 15(d) that for anchoring strengths $\epsilon_d=0.0$ (no anchoring influence at the top

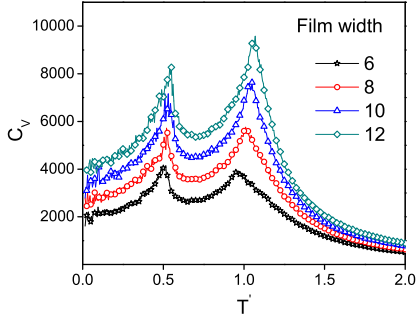


Figure 13: Comparison of variations of the specific heat C_v as a function of temperature in films of thickness d (in lattice units) = 6 (stars), 8 (circles), 10 (upward triangles) and 12 (diamonds), in Type-B film.

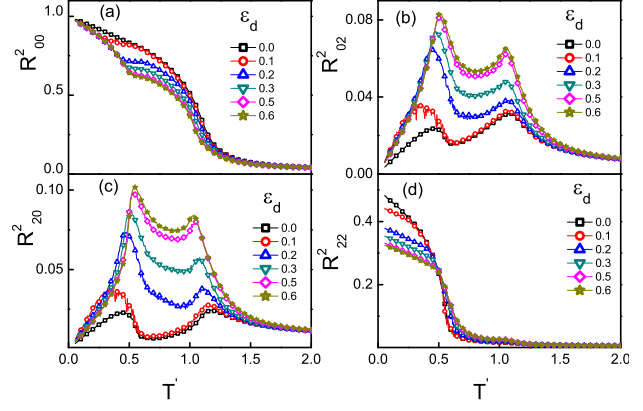


Figure 15: Variation of order parameters with temperature for different anchoring strengths (ϵ_d) in Type-A film of thickness 8 lattice units: (a) R^2_{00} (b) R^2_{02} (c) R^2_{20} and (d) R^2_{22} .

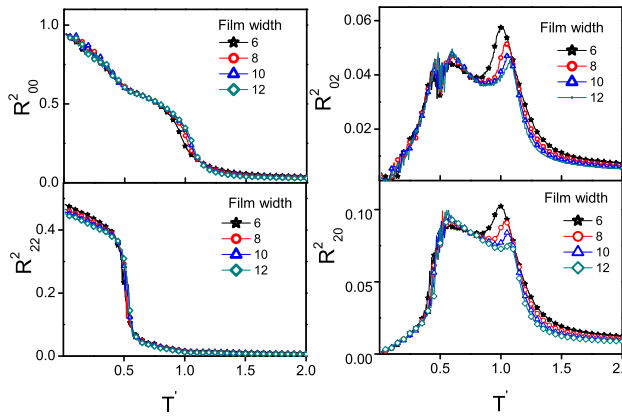


Figure 14: Comparison of variation of order parameters with temperature for different film thickness (d) in Type-B film.; $d = 6$ (stars), $d = 8$ (circles), $d = 10$ (upward triangles) and $d = 12$ (diamonds)

substrate) and for a low value of $\epsilon_d = 0.1$, the uniaxial order R^2_{00} and the biaxial order R^2_{22} attain maximum values of 1.0 and 0.5, respectively, - for example without the characteristic features observed earlier (with $\epsilon_d = 1$) at the onset of the N_B phase. Their variations are similar to bulk LC systems without confining surfaces (see Fig. 2). For $\epsilon_d \geq 0.2$ the primary director assumes a bent structure and the primary order is constrained with an upper bound of 0.8 for $\epsilon_d = 0.2$ in the uniaxial nematic phase. A similar sharp difference is exhibited by R^2_{22} as well, and its temperature variation qualitatively changes above the threshold value of $\epsilon_d = 0.2$. The order parameters R^2_{02} and R^2_{20} , shown in Fig. 15(b) and (c), start with very low values at $\epsilon_d = 0.0$ and 0.1, but increase significantly for higher anchoring strength ($\epsilon_d \geq 0.2$). Thus it appears that a minimum threshold anchoring strength ($\epsilon_d \geq 0.2$) is necessary for the film to exhibit the curious structures, reported earlier, arising from the bent formation of its director. The progressive development of this scenario with increase of ϵ_d is evident from the gradual decrease of the system primary order (Fig. 15(a)) in the uniaxial phase.

Fig. 16 depicts the anchoring transition in a Type-B film. It is to be noted (Fig. 16(a)) that though the anchoring transition is observed for $\epsilon_d \geq 0.2$, the primary director displays a prominent bent director structure for values of $\epsilon_d \sim 0.6$. The variation of R^2_{22} , R^2_{02} and R^2_{20}

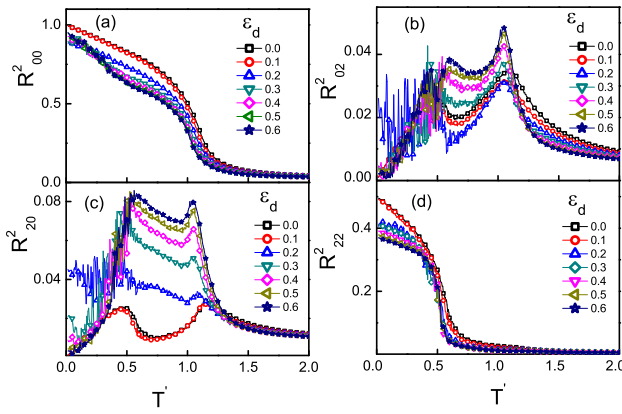


Figure 16: Variation of order parameters with temperature for different anchoring strengths (ϵ_d) in Type-B film of thickness 8 lattice units: (a) R_{00}^2 (b) R_{02}^2 (c) R_{20}^2 and (d) R_{22}^2 .

(shown in Figs. 16 (b) - Fig. 16(d)) is similar to that for the Type-A film, except that fluctuations are large at the anchoring transition, especially for R_{02}^2 and R_{20}^2 .

4. Conclusions

Equilibrium director structures in thin planar films of biaxial LC medium, imposing strong hybrid anchoring conditions at the two substrates on the molecular long axes (z -axes), are investigated through Monte Carlo simulation, (Boltzmann sampling) based on a Hamiltonian model under dispersion approximation (at $\lambda_d = 0.35$). Geometrical confinement induces a small degree of biaxial order in the intermediate phase, whereas unconfined bulk system in this phase has uniaxial symmetry. We refer to this intermediate phase, which is essentially uniaxial with inhomogeneous distribution of biaxial order as N'_U . Type-A film is coupled to the substrate only via the molecular long axes (z -axes), while in Type-B film the LC molecules interact with the substrate involving the three molecular axes. Detailed MC simulational studies are carried out on these films covering both the mesophases, focussing on the temperature variation of the director structures, both of bulk film as well as its layers. A comparative analysis of the data shows that the primary director, defined by the ordering of the molecular z -axes and constrained in a

plane perpendicular to the substrates, changes its role as the direction of maximal order qualitatively. In the biaxial phase, the maximum orientational ordering arises from the minor molecular axes (y -axes in the case of Type-A film and x -axes in the case of Type-B film). This order is contained in the plane of the substrates, and it develops towards its unhindered maximum value of unity as the system is cooled in the biaxial phase. This shows that geometrical constraints, and hence consequent averaging over the layers, are no more at play in this phase. We also find large fluctuations of this major order in Type-B film, unaccounted by typical MC error estimates (exceeding by an order of magnitude). Our further studies with multiple initial random configurations, show that Type-B film perhaps hosts shallow free energy minimum with several local minima (like glass structure), and hence forced to giving rise to non-unique MC averages depending on the trajectory in the configuration space. This is clearly due to the frustration induced in the Type-B system under the simultaneous influence of hybrid anchoring conditions affecting the minor axes on one hand, and the ordering effect on them due to the Hamiltonian at the onset of the biaxial phase on the other. These are borne out by the observed fluctuations in this film in the angles of the primary director of different layers. Such effects are not seen in Type-A film, which displays a unique MC average value, independent of the trajectory of the MC evolution. We conclude that the Type-A film has a very stable in-plane dominant ordering, in comparison to Type-B film. Further, its anchoring conditions, imposing only on the molecular long axes, are more readily realizable in a laboratory. Both the systems are rather insensitive to the film thicknesses. We also find that the relative variation of anchoring strengths plays a role in inducing the above confinement effects. The anchoring induced transition observed while tuning these parameters suggests that a minimum threshold anchoring strength is necessary to realize these in-plane structures in the biaxial nematic phases.

5. Acknowledgments

The simulations are carried out in the Centre for Modelling Simulation and Design (CMSD) at the University of Hyderabad. BKL acknowledges the financial support of University Grants Commission of India for the grant of a research fellowship.

References

- [1] M. J. Freiser, Phys. Rev. Lett. 24 (1970) 1041 .
- [2] B. R. Acharya, A. Primak, T. J. Dingemans, E. T. Samulski, S. Kumar, Pramana 61 (2003) 231.
- [3] B. R. Acharya, A. Primak, S. Kumar, Phys. Rev. Lett. 92 (2004) 1455061.
- [4] L. A. Madsen, T. J. Dingemans, M. Nakata, E. T. Samulski, Phys. Rev. Lett. 92 (2004) 145505.
- [5] K. Merkel, A. Kocot, J. K. Vij, R. Korlacki, G. H. Mehl, T. Meyer, Phys. Rev. Lett. 93 (2004) 237801.
- [6] J. L. Figueirinhas, C. Cruz, D. Filip, G. Feio, A. C. Ribeiro, Y. Frere, T. Meyer, G. H. Mehl, Phys. Rev. Lett. 94 (2005) 107802.
- [7] K. Neupane, S. W. Kang, S. Sharma, D. Carney, T. Meyer, G. H. Mehl, D. W. Allender, S. Kumar, S. Sprunt, Phys. Rev. Lett. 97 (2006) 207802.
- [8] F. Hessel H. Finkelmann, Polym. Bull. 15 (1996) DOI:10.1007/BF00254854.
- [9] K. Severing and K. Saalwachter, Phys. Rev. Lett. 92 (2004) 125501.
- [10] J. H. Lee, T. K. Lim, W. T. Kim, J. I. Jin, J. Appl. Phys. 101 (2007) 034105.
- [11] M. Nagaraj, Y. P. Panarin, U. Manna, J. K. Vij, C. Keith, C. Tschierske, Appl. Phys. Lett. 96 (2010) 0111106.
- [12] C. Tschierske D. J. Photinos, J. Mat. Chem. 20 (2010) 4263.
- [13] K. Van Le, M. Mathews, M. Chambers, J. Harden, Q. Li, H. TakeZoe, A. Jakli, Phys. Rev. E. 79 (2009) 030701(R) .
- [14] T. Ostapenko, C. Zhang, S. N. Sprunt, A. Jakli, J. T. Gleeson, Phys. Rev. E 84 (2011) 021705 .
- [15] A. M. Sonnet, E. G. Virga, and G. E. Durand, Phys. Rev. E **67**, 061701 (2003).
- [16] G. De Matteis, and E. G. Virga, Phys. Rev. E **71**, 061703 (2005).
- [17] F. Bisi, E. G. Virga, E. C. Gartland Jr., G. De Matteis, A. M. Sonnet, and G. E. Durand, Phys. Rev. E **73**, 051709 (2006).
- [18] F. Bisi, S. Romano, E. G. Virga, Phys. Rev. E **75**, 041705 (2007).
- [19] G. De Matteis, F. Bisi, and E. G. Virga, Continuum. Mech. Thermodynamics. **19**, 1 (2007).
- [20] F. Bisi, G. R. Luckhurst, E. G. Virga, Phys. Rev. E **78**, 021710 (2008).
- [21] R. Berardi, L. Muccioli, S. Orlandi, M. Ricci, C. Zannoni, J. Phys.: Condens. Matter. 20 (2008) 463101.1.
- [22] G. De Matteis and S. Romano, Phys. Rev. E **78**, 021702 (2008).
- [23] B. Kamala Latha, Regina Jose, K. P. N. Murthy and V. S. S. Sastry, Phys. Rev. E **89**, 050501(R) (2014).
- [24] B. Kamala Latha, Regina Jose, K. P. N. Murthy and V. S. S. Sastry, Phys. Rev. E **92**, 012505 (2015).
- [25] R. Berardi, L. Muccioli, C. Zannoni, J. Chem. Phys. 128 (2008) 024905.
- [26] G. R. Luckhurst, Thin Solid Films 393 (2001) 40.
- [27] P. Sheng, Phys. Rev. Lett. 37 (1976) 1059; Phys. Rev. A 26 (1982) 1610.
- [28] G. Barbero, R. Barberi, J. Phys.(Paris) 44 (1983) 609.
- [29] G. Sai Preeti, Ph.D Thesis, Monte Carlo Study of Confined Liquid Crystals: Films, Droplets and Biaxial nematics, University of Hyderabad, India, 2009.
- [30] P. Pasini, C. Chiccoli C. Zannoni in P. Pasini, C. Zannoni (Eds.), Advances in computer simulations of liquid crystals, Kluwer Acad. Publishers, 2005.
- [31] F. Biscarini, C. Chiccoli, P. Pasini, F. Semeria C. Zannoni, Phys. Rev. Lett. 75 (1995) 1803.
- [32] R. J. Low, Eur. J. Phys. 23 (2002) 111.
- [33] M. H. Quenonille, Biometrika **43**, 353 (1956).

[34] J. Shao, D. Tu, The Jackknife and Bootstrap, Springer, New York, 1995.

[35] S. D. Peroukidis, P. K. Karahaliou, A. G. Vanakaras, D. J. Photinos Liq. Cryst. 36:6, 727 (2009).